Pion double charge exchange on the even selenium isotopes

P. Hui, H.T. Fortune, M.A. Kagarlis,* and J.M. O'Donnell†
University of Pennsylvania, Philadelphia, Pennsylvania 19104

A.R. Fazely‡
Louisiana State University, Baton Rouge, Louisiana 70803

R. Gilman
Rutgers, The State University of New Jersey, Piscataway, New Jersey 08855

S. Mordechai
Ben Gurion University of the Negev, Beer Sheva 84105, Israel

D.L. Watson
University of York, York Y01 5DD, United Kingdom
(Received 30 January 1995)

Pion-induced double charge exchange (π^+,π^-) on ^{76,78,80,82}Se, leading to the double isobaric analog states (DIAS) and the ground states of ^{76,78,80,82}Kr, has been studied at a laboratory angle of 5° and incident pion kinetic energy of 293.2 MeV. Cross sections for these transitions have been extracted, and those for the DIAS are compared to two simple models of pion double charge exchange.

PACS number(s): 25.80.Gn, 27.50.+e

I. INTRODUCTION

The pion double charge exchange reaction (π^+,π^-) on a nucleus is a process that must involve two nucleons in lowest order. As such, it is a useful probe to study two-nucleon correlations in nuclei. In recent years, there have been several experiments to investigate these two-nucleon correlations by studying the sensitivity of pion double charge exchange (DCX) cross sections to neutron excess. Chains of isotopes were used for such a purpose, including calcium [1–4], nickel [5, 6], and tellurium isotopes [7, 8]. Simple theoretical models of transitions to the double isobaric analog states (DIAS) and to the ground states (g.s.) of the residual nuclei have been presented [9–13]. Forward-angle cross sections for the DIAS transition approximately follow an $A_{\rm tgt}^{-10/3}$ mass dependence [10], as predicted by the model of Johnson and Siciliano [9]. For Ca and Ni isotopes, the seniority models adequately accounted for some of the data at low incident pion energy and at $T_\pi \approx 293$ MeV [11, 13, 14].

In the chain of naturally occurring selenium isotopes, the neutron number varies from 42 to 48, which is from near the middle of the $N = 28$–50 shell to near the $N = 50$ closed shell. Therefore one might expect dramatic changes in nuclear structure within the chain of selenium isotopes, more than in other chains of isotopes in the medium mass region. It is interesting to investigate whether this change has an effect on pion DCX cross sections. In this paper, we report results of an experiment which measured the forward-angle cross sections for ^{76,78,80,82}Se$(\pi^+,\pi^-)^{76,78,80,82}$Kr, leading to the DIAS and the g.s. of krypton isotopes, and we compare the DIAS cross sections to some of the models mentioned above.

II. EXPERIMENTAL PROCEDURE AND DATA ANALYSIS

The experiment was performed at the Clinton P. Anderson Meson Physics Facility (LAMPF), using the Energetic Pion Channel and Spectrometer (EPICS). Details of the setup of EPICS for pion DCX experiments have been published elsewhere [15, 16]. The measurements were made at a laboratory angle of 5° with 293.2 MeV incident pion kinetic energy. The targets used included five cells of isotopic selenium and four cells of natural selenium. Several cells were placed in the beam simultaneously at any one time. Three different target configurations were used during the experiment, as shown in Figs. 1(a)–1(c).

For each isotopic target cell, the target material, in the form of elemental powder, was placed in a Mylar envelope that was attached to an aluminum frame, as shown in Fig. 1(d). The target powder did not fill the envelope volume in any of the target cells. There was one cell

*Present address: Niels Bohr Institute, Blegdamsvej 17, DK 2100 Copenhagen, Denmark.
†Present address: Los Alamos National Laboratory, Los Alamos, NM 87545.
‡Present address: Department of Physics, Southern University, Baton Rouge, LA 70813.

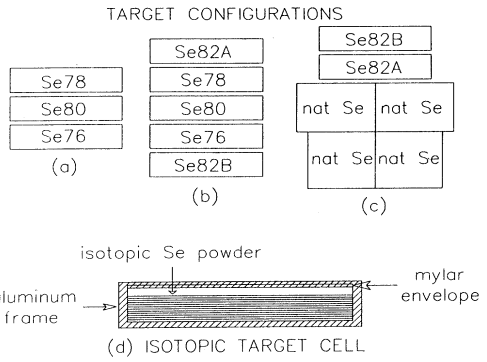

FIG. 1. Configurations of the selenium target cells during the experiment (a)–(c); sketch of a typical isotopic selenium target cell (d).

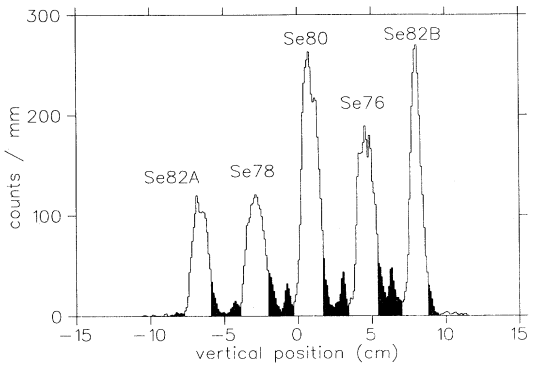

FIG. 2. A histogram of (π^+, π^-) events vs their vertical positions on the target, with the target configuration of Fig. 1(b). The shaded regions indicate possible events from the aluminum frames. Note that positive x corresponds to downward direction.

for each of the ^{76}Se, ^{78}Se, and ^{80}Se targets, and enough material to construct two target cells for ^{82}Se (referred to as Se76, Se78, Se80, Se82A, and Se82B, respectively, in Fig. 1 and in Table I). The areal density of each isotopic Se target was about 0.6 g/cm^2, and the isotopic enrichment in each cell was greater than 96%. The areal density of the aluminum frame was about 0.214 g/cm^2, and that of the Mylar envelope was about 0.002 g/cm^2 on each side (0.004 g/cm^2 total in the beam).

The natural selenium powder was placed in four rectangular cells with nickel walls [referred to as "nat Se" in Fig. 1(c)]. The average areal density of ^{nat}Se was about 2.13 g/cm^2, while the nickel cell walls had an average areal density of 0.09 g/cm^2 in the beam (front and back walls total). The purity of ^{nat}Se target powder was about 99%, and the relative abundances of various Se isotopes in natural selenium are roughly 9% for ^{76}Se, 8% for ^{77}Se, 24% for ^{78}Se, 50% for ^{80}Se, and 9% for ^{82}Se [17]. Pion DCX on ^{nat}Se had been investigated in a previous experiment [18], and it was included in this experiment for calibration purposes only.

Displayed in Fig. 2 is an x-target histogram (x is vertical at EPICS) for the target configuration shown in Fig. 1(b). It is clear that with target cuts in software, the events from each Se isotope are easily separated from those of the other isotopes and from those coming from the top part of its aluminum frame. It is more difficult to separate the events of interest from those due to the bottom part of the aluminum frame. However, in Fig. 3 we show a spectrum of DCX events for one Se isotope and a spectrum of DCX events from the top part of the aluminum frame of the same target cell. Since the top and bottom of the aluminum frame have about the same areal density, we expect about the same rate of events from each. As shown in Fig. 3, the top part of the aluminum frame contributed few DCX events in the g.s. and DIAS regions. Therefore we expect negligible background events from the bottom part as well.

Absolute normalizations were obtained from π-p scattering from a CH_2 target of areal density 25.8 mg/cm^2 and comparing the yields with cross sections calculated from π-nucleon phase shifts [19]. Target cuts in software were made during the analysis of the CH_2 data, in order to match the areas and positions of the π-p events with those of the Se events. The acceptance of the spec-

TABLE I. Target information.

Target cell	Purity (%)	Areal density (g/cm^2)
Se76	96.88	0.625
Se78	98.58	0.566
Se80	99.45	0.616
Se82A	96.81	0.714
Se82B	96.81	0.542

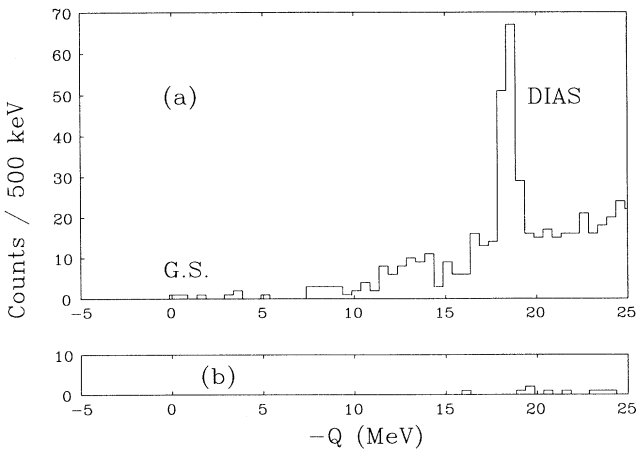

FIG. 3. (a) A spectrum of ^{80}Se$(\pi^+, \pi^-)^{80}$Kr at 5° and at the incident pion kinetic energy of 293.2 MeV; (b) a spectrum of DCX events during the same runs from the top part of the aluminum frame of the Se80 target cell.

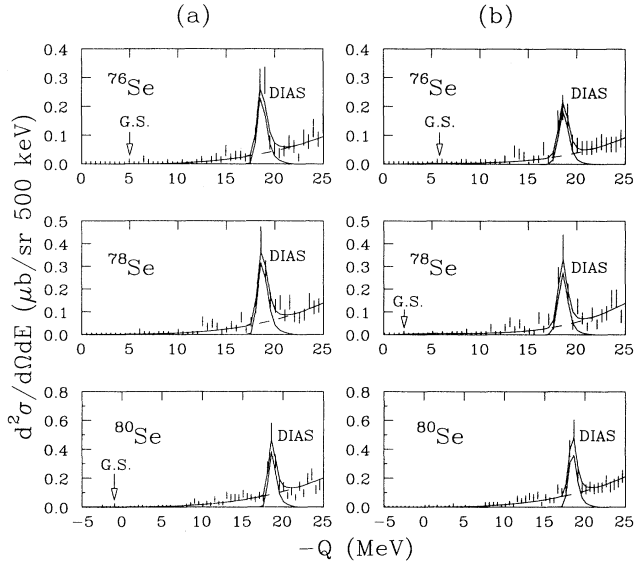

FIG. 4. Spectra of ^{76,78,80}Se$(\pi^+,\pi^-)^{76,78,80}$Kr at 5° and at the incident pion kinetic energy of 293.2 MeV, with (a) the targets in the configuration of Fig. 1(a), and (b) the targets in the configuration of Fig. 1(b). The histograms are absolutely normalized and acceptance-corrected. The error bars are statistical only.

trometer was determined from pion inelastic scattering on ^{12}C at a laboratory angle of 33° and T_π = 180 MeV, by varying the spectrometer field to cover an outgoing pion momentum range of about ±8% of the central momentum of the spectrometer. Elastic (π^+,π^+) scattering was done on the Se targets to obtain peak shapes to use in the data analysis. Elastic peak widths were about 700 keV [full width at half maximum (FWHM)], primarily arising from target thickness.

Normalized and acceptance-corrected histograms for every isotopic Se target in every target geometry were generated and analyzed with the code NEWFIT [20]. These spectra are displayed in Figs. 4 and 5. The DIAS peaks were apparent in these spectra, and they were fitted with peak shapes taken from elastic scattering. Following standard practice in analyzing pion DCX data, the background was assumed to be described by a third-order polynomial in Q [21,22]. There were a few events at the locations corresponding to the Kr ground states, and they were analyzed by summing the normalized yields in the regions of interest.

III. DISCUSSION OF RESULTS

For each Se isotope, the DIAS cross sections extracted from the data sets corresponding to different target cells or different target configurations are plotted together in Fig. 6. The results from various data sets are consistent. In Table II, we quote the weighted averages of these cross sections and their Q values measured in this experiment. The statistical uncertainties in the DIAS cross sections are about 8% on average, and the systematic uncertainties (mainly due to uncertainties in normalization introduced via target cuts in software during the analysis of CH_2 data and uncertainties in fitting the background) are about 6% on average. The uncertainties quoted in Table II are the statistical and systematic uncertainties added in quadrature.

The measured ground-state cross sections and Q values

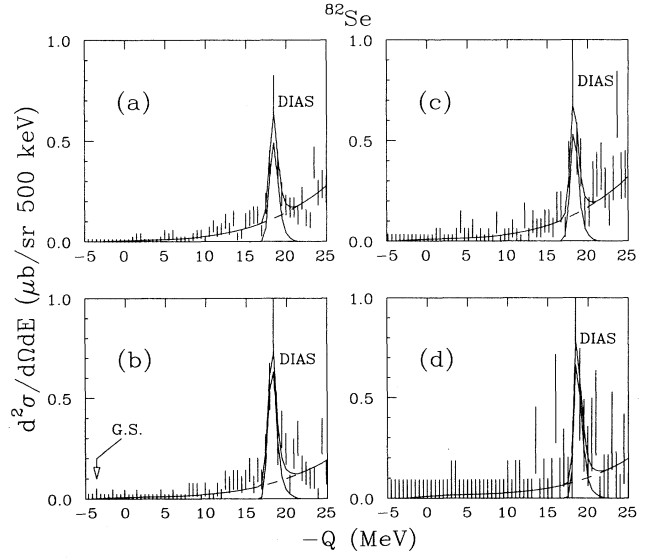

FIG. 5. Spectra of ^{82}Se$(\pi^+,\pi^-)^{82}$Kr at 5° and at the incident pion kinetic energy of 293.2 MeV, with (a) and (b) from the target cells Se82A and Se82B, respectively, in the target configuration of Fig. 1(b), and with (c) and (d) from the target cells Se82A and Se82B, respectively, in the target configuration of Fig. 1(c). The histograms are absolutely normalized and acceptance-corrected. The error bars are statistical only.

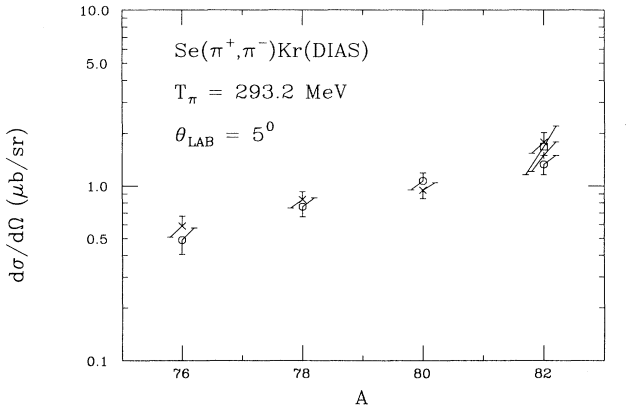

FIG. 6. The DIAS cross sections extracted from the data sets of various Se targets in various target configurations. The diagonal crosses are from the targets in the configuration of Fig. 1(a) and from the target cell Se82B in the configuration of Fig. 1(b). The circles are from the rest of the targets in the configuration of Fig. 1(b). The vertical cross and the square are from the target cells Se82A and Se82B, respectively, in the configuration of Fig. 1(c).

TABLE II. Differential cross sections for Se(π^+,π^-)Kr(DIAS) at $T_\pi = 293.2$ MeV, $\theta_{\rm lab} = 5°$.

	-$Q_{\rm DIAS}$(MeV)		$\sigma_{\rm DIAS}(\mu$b/sr)		
$A_{\rm tgt}$	Calc.[a]	Expt.[b]	Expt.[b]	Model I[c]	Model II[d]
76	19.08	18.74 ± 0.08	0.547 ± 0.073	0.557	0.557
78	18.87	18.82 ± 0.06	0.802 ± 0.081	0.824	0.760
80	18.68	18.66 ± 0.06	1.00 ± 0.10	1.113	1.073
82	18.49	18.50 ± 0.11	1.52 ± 0.15	1.416	1.458

[a]From systematics of Coulomb displacement energies. See Ref. [24].
[b]Measured in this work.
[c]Predicted by a simple mass-dependence model [10]. See text for discussion.
[d]Predicted by the generalized seniority model [12, 13]. See text for discussion.

are listed in Table III. We note that the g.s. cross sections are small compared to the DIAS cross sections.

A. Simple mass-dependence model

We now turn to the comparison between our DIAS data and two simple models of pion double charge exchange. The first model that we compare with is the result of a fit to previous DCX DIAS data at $T_\pi = 293$ MeV [10]. It predicts that near 293 MeV, the 5° DIAS cross section is given by

$$\frac{d\sigma}{d\Omega}(A_{\rm tgt}) = 0.068(N-Z)(N-Z-1)\left(\frac{A_{\rm tgt}}{42}\right)^{-3.24} \mu\text{b/sr}. \quad (1)$$

We note that the factor $(N-Z)(N-Z-1)$ simply counts the number of pairs of excess neutrons without any assumption of correlations. In Table II, we list the DIAS cross sections predicted by expression (1) for the Se isotopes, and we display this predicted mass dependence (solid curve) along with our data in Fig. 7. It is clear that this systematic trend describes the Se data rather well. (The total χ^2 is 1.85.) This result is somewhat surprising, since this systematic trend was derived by fitting the data of many different nuclei without regard for nuclear structure, and we had not expected it to hold in the Se mass region, where nuclear structure is changing rapidly.

TABLE III. Differential cross sections for Se(π^+,π^-) Kr(g.s.) at $T_\pi = 293.2$ MeV, $\theta_{\rm lab} = 5°$.

	-$Q_{\rm g.s.}$ (MeV)		
$A_{\rm tgt}$	Calc.[a]	Expt.[b]	$\sigma_{\rm g.s.}(\mu$b/sr)[b]
76	5.27	5.35 ± 0.47	0.014 ± 0.008
78	1.86	2.08[c]	0.006 ± 0.006
80	-1.15	-1.47 ± 0.50	0.017 ± 0.010
82	-4.02	-3.64[c]	0.013 ± 0.013

[a]Deduced from the values of mass excesses in the literature [25].
[b]Measured in this work.
[c]One event observed.

B. Generalized seniority model

A second model that has been compared to data on a chain of isotopes is a model of pion DCX that assumes that the mass region in question has good generalized seniority [12]. It predicts that the DIAS cross section is given by

$$\frac{d\sigma}{d\Omega}(\text{g.s.}; T = T_Z = n \rightarrow \text{DIAS}; T = n, T_Z = n-2)$$

$$= \left[\frac{A_0}{A_{\rm tgt}}\right]^c n(2n-1)\left|\alpha + \frac{\beta}{(2n-1)}\right|^2, \quad (2)$$

where n is the number of pairs of excess neutrons, and the complex amplitudes α and β are assumed to be independent of n and $A_{\rm tgt}$. The exponent c is expected to be in the range of 2.33–4.04, and A_0 is a typical mass number within the mass region in question ($A_0 = 80$ in our case).

This generalized seniority model has been successful in accounting for the Ni DCX data [5, 13]. A simpler (single-orbital) version adequately describes the Ca data

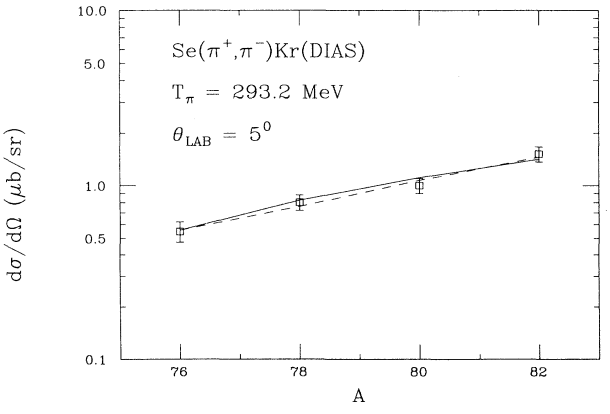

FIG. 7. The DIAS cross sections measured in this work. The solid and dashed curves result from the predictions of a simple mass-dependence model and of the generalized seniority model, respectively (see text for discussion).

TABLE IV. Parameters of the generalized seniority model fitted to Se(π^+, π^-)Kr(DIAS) data. See text for discussion.

c	$\lvert\alpha\rvert$ ($\sqrt{\mu b/sr}$)	$\lvert\beta\rvert$ ($\sqrt{\mu b/sr}$)	cos ϕ	χ^2
0.00	0.154 ± 0.061	1.04 ± 0.85	-0.57 ± 0.47	0.83
2.33	0.176 ± 0.063	1.15 ± 0.85	-0.70 ± 0.29	0.91
3.33	0.184 ± 0.056	1.19 ± 0.78	-0.74 ± 0.21	0.96
4.04	0.190 ± 0.053	1.24 ± 0.71	-0.76 ± 0.18	0.99

[11]. We are therefore motivated to try it on our Se data, even though generalized seniority may not be good in the Se mass region. There is some indication [23] that expression (2) may have wider validity than the generalized seniority assumed in its derivation. To extract α and β, we fitted expression (2) to our DIAS data. The fitted parameters are not sensitive to reasonable variation in the exponent c, given the uncertainties in our data. For various values of c, we obtained similar values for $|\alpha|, |\beta|$, and cos ϕ (ϕ is the relative phase between α and β), as listed in Table IV. With $c = 4.04$, we obtained $|\alpha| = 0.190 \pm 0.053$ $\sqrt{\mu b/sr}$, $|\beta| = 1.24 \pm 0.71$ $\sqrt{\mu b/sr}$, and cos $\phi = -0.76 \pm 0.18$. With these magnitudes and phase, we derived the dashed curve shown in Fig. 7 (the values of theoretical cross sections are listed in Table II). Thus the selenium DIAS data are consistent with expression (2).

The generalized seniority model also relates the g.s. cross sections to the DIAS cross sections, but for several active orbitals it assumes that there is only one kind of valence nucleon in the target nucleus. Since this is not true for the Se isotopes (there are six valence protons in addition to the valence neutrons), we do not attempt to compare our g.s. data to the model here.

IV. CONCLUSION

The cross sections of pion double charge exchange on ^{76,78,80,82}Se at a laboratory angle of 5° and incident pion kinetic energy of 293.2 MeV, leading to the DIAS and to the ground states of ^{76,78,80,82}Kr, have been measured. The DIAS data are consistent with a simple mass-dependence model and with a general expression derived first for the generalized seniority model. Further work is necessary to understand the small g.s. cross sections. The DIAS cross sections do not seem to be sensitive to dramatic changes in the nuclear structure in the Se mass region, and no trend is evident in the g.s cross sections given the limited statistics of the data. In the future, it would be interesting to study these at lower incident energy closer to the Δ_{33} resonance. The g.s. cross sections are larger in that energy region [18] with better chances of improved statistics, and the DIAS cross sections may be more sensitive to nuclear structure effects.

ACKNOWLEDGMENTS

We acknowledge interesting discussions with J. N. Ginocchio. We thank Oak Ridge National Laboratory for providing us the enriched selenium isotopes. Financial support was provided by the National Science Foundation and the Department of Energy.

[1] L. C. Bland, R. Gilman, M. Carchidi, K. Dhuga, C. L. Morris, H. T. Fortune, S. J. Greene, P. A. Seidl, and C. F. Moore, Phys. Lett. **128B**, 157 (1983).
[2] M. J. Leitch *et al.*, Phys. Lett. B **294**, 157 (1992).
[3] P. A. Seidl *et al.*, Phys. Rev. C **42**, 1929 (1990).
[4] Z. Weinfeld, E. Piasetzky, M. J. Leitch, H. W. Baer, C. S. Mishra, J. R. Comfort, J. Tinsley, and D. H. Wright, Phys. Lett. B **237**, 33 (1990).
[5] D. R. Benton, H. T. Fortune, J. M. O'Donnell, R. Crittenden, M. McKinzie, E. Insko, R. Ivie, D. A. Smith, and J. D. Silk, Phys. Rev. C **47**, 140 (1993).
[6] H. T. Fortune, G. B. Liu, J. M. O'Donnell, J. D. Silk, and S. Mordechai, Phys. Rev. C **50**, 306 (1994).
[7] A. Fazely *et al.*, Phys. Lett. B **208**, 361 (1988).
[8] D. A. Smith, H. T. Fortune, G. B. Liu, J. M. O'Donnell, M. Burlein, S. Mordecahi, and A. R. Fazely, Phys. Rev. C **46**, 477 (1992).
[9] M. B. Johnson and E. R. Siciliano, Phys. Rev. C **27**, 730 (1983); **27**, 1647 (1983).
[10] R. Gilman *et al.*, Phys. Rev. C **35**, 1334 (1987).
[11] N. Auerbach, W. R. Gibbs, J. N. Ginocchio, and W. B. Kaufmann, Phys. Rev. C **38**, 1277 (1988).
[12] J. N. Ginocchio, Nucl. Phys. **A560**, 321 (1993).
[13] J. N. Ginocchio, Phys. Rev. C **48**, 1460 (1993).
[14] J. D. Zumbro *et al.*, Phys. Rev. C **36**, 1479 (1987).
[15] S. J. Greene, Ph.D. thesis, University of Texas at Austin, Los Alamos National Laboratory Report No. LA-8891-T, 1981.
[16] S. J. Greene *et al.*, Phys. Rev. C **25**, 927 (1982).
[17] *CRC Handbook of Chemistry and Physics*, 1st student ed. (CRC Press, Boca Raton, FL, 1988), p. B-128.
[18] P. Hui, H. T. Fortune, R. Gilman, C. M. Laymon, J. D. Zumbro, P. A. Seidl, and J. A. Faucett, Phys. Rev. C **49**, 83 (1994).
[19] G. Rowe, M. Salomon, and R. H. Landau, Phys. Rev. C **18**, 584 (1978).
[20] C. L. Morris, computer code NEWFIT (unpublished).
[21] S. Mordechai *et al.*, Phys. Rev. Lett. **60**, 408 (1988).
[22] S. Mordechai *et al.*, Phys. Rev. C **40**, 850 (1989).
[23] D. A. Smith (private communication).
[24] J. M. O'Donnell, H. T. Fortune, J. D. Silk, S. Mordechai, C. L. Morris, J. D. Zumbro, S. H. Yoo, and C. F. Moore, Phys. Rev. C **46** 2259 (1992).
[25] A. H. Wapstra, G. Audi, and R. Hoekstra, At. Data Nucl. Data Tables **39**, 281 (1988).